

Sylwester SAMBORSKI¹, Michał KALISZUK¹, Tomasz ŁUSIAK², Dariusz KASPEREK³
Katarzyna SZWEDZIAK⁴, Żaneta PRUSKA⁴

¹The Lublin University of Technology, Mechanic Faculty, Chair of Applied Mechanics

²The Polish Air Force Academy in Dęblin, Faculty of Aviation, Chair of Airframe and Engine

³URSUS BUS S.A., Lublin, Poland

⁴The Opole University of Technology, Faculty of Production Engineering, Chair of Biosystems Engineering

e-mail: s.samborski@pollub.pl, kaliszuk.m@vp.pl, t.lusiac@wsosp.pl, dariusz.kasperek@ursus.com,

k.szwedziak@po.opole.pl, z.pruska@po.opole.pl

NUMERICAL ANALYSIS OF FRONT AXLE BRACKET STRENGTH IN FARM TRACTOR

Summary

This paper describes strength evaluation for D4CS4 FA20.25 bracket, mounted in tractors of the URSUS Company. The analysis was based on stress modelling, supported by the finite element method (FEM). It was assumed in the model that the studied element was made of ductile cast iron and subject to three forces at three support points. Stress distribution simulations were run for various boundary conditions in order to identify the areas most exposed to cracking hazards. On this basis, engineering changes were introduced to increase the mechanical strength of the bracket with maximum cost-effectiveness of its production.

Key words: numerical modelling, finite element method, axle bracket, stress distribution, bracket of agricultural tractor

NUMERYCZNA ANALIZA WYTRZYMAŁOŚCIOWA WSPORNIKA OSI PRZEDNIEJ CIĄGNIKA ROLNICZEGO

Streszczenie

W artykule opisano analizę wytrzymałościową wspornika D4CS4 FA20.25 montowanego w ciągnikach firmy URSUS. Analizę przeprowadzono w oparciu o modelowania naprężeń metodą elementów skończonych (MES). W modelu założono, że element badany jest wykonany z żeliwa sferoidalnego, który był obciążony trzema siłami w trzech punktach podparcia. Przeprowadzono symulacje rozkładu naprężeń dla różnych warunków brzegowych w celu wyodrębnienia obszarów najbardziej narażonych na pękanie. Na tej podstawie wprowadzono zmiany konstrukcyjne, zwiększające wytrzymałość wspornika przy minimalizacji kosztów jego wykonania.

Słowa kluczowe: modelowanie numeryczne, metoda elementów skończonych, wspornik osi, rozkład naprężeń, wspornik ciągnika rolniczego

1. Introduction

Project design procedures of various machine parts and components often require simulation tests to identify zones, most exposed to the highest load and stress impacts. It is associated with formulation of different tension hypotheses, which would describe the behaviour of applied structural materials subject to complex loads. Such hypotheses, as the hypothesis of the highest tensile stress or the hypothesis of the highest normal stress, proved very useful at the time when stone, i.e., a brittle material, was the primary construction material [2, 4, 13, 15]. Over the past two centuries, two hypotheses were commonly used, namely: Coulomb-Tresca hypothesis of maximum shear stresses and another one referring to the specific energy (of Huber-Hencky-von Mises), which enable users to obtain good compliance with experimental data for metal alloys and steels [9, 13]. There are also many hypotheses, developed for modern materials, e.g. for composite laminates, which clearly indicate a growing application trend. These hypotheses include, among others: the Azzi-Trasi-Hill failure criterion or the Tsai-Wu criterion [1, 5, 10, 19]. Selection of an appropriate tension hypothesis/failure criterion depends on the type of material, used for production of a given structural element, while a number of available computer programs, based on the Finite Element Method (FEM), allow for implementation practically of every known hypothesis [10]. This paper presents application of the largest strain hypothesis for a structural element, made of iron, as

well as simulation results were analysed (with maps of reduced stresses and strains). The simulation was aimed to identify the areas most exposed to damage hazards during operation and engineering revisions were proposed to increase mechanical strength with maximum cost-effectiveness of the element manufacturing process. The element of study was a D4CS4-FA20.25 front axle bracket, used in URSUS C-380M agricultural tractors (Fig. 1).



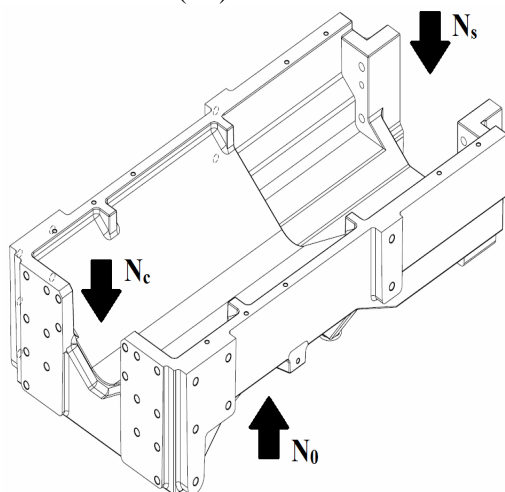
Source: own work/ Źródło: opracowanie własne

Fig. 1. D4CS4-FA20.25 front axle bracket of URSUS C-380M tractor with a mounted axle

Rys. 1. D4CS4-FA20.25 przednia oś wspornika ciągnika URSUS C-380M z zamontowaną osią

Figure 2 illustrates the bracket mounting configuration on the front axle of the tractor. A four-cylinder engine was mounted to the bracket sides, together with dead weights to provide an additional load for the front axle of the tractor. The bracket was then a structural element which, in the course of normal tractor operation, was often subject to damage due to handling of high loads. The loads, taken into account in a numerical evaluation of the D4CS4-FA20.25 bracket, included the loads, resulting from the front axle reactions, the engine mass and the frontal dead weights, mounted to the analysed brackets.

Figure 2 presents the points to which the bracket loading forces were applied. It was assumed that the bracket was impacted by the following three primary forces: the engine weight (N_s), the weight of dead weights (N_c) and the front axle reaction (N_0).



Source: own work/ Źródło: opracowanie własne

Fig. 2. Distribution of forces acting on D4CS4-FA20.25 bracket

Rys. 2. Rozkład sił działających na wspornik D4CS4-FA20.25

2. Tension hypothesis

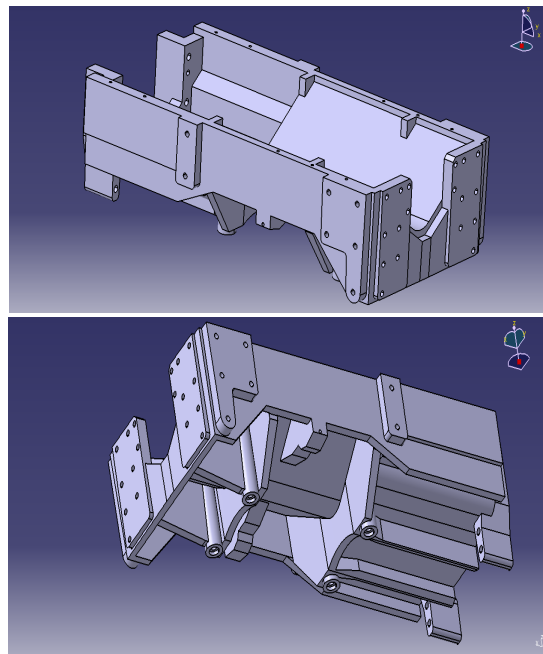
Numerical calculations were carried out in the ABAQUS environment. It is a software package which enables stress distribution simulation. The calculation software employed the finite element method (FEM). This method enables individual material characteristics to be used in calculations together with generation of complex calculation grids [18]. A material model for ductile iron was defined for numerical processing, its properties being compliant with 0.7040 (EN-GJS-400-15) standard [14]. This type of material consists of iron with modular graphite. The material maintains iron characteristics but, due to graphite contents, its mechanical strength is close to that of steel (Table 1).

Table 1. Material data of D4CS4-FA20.25 bracket
Tab. 1. Dane materiałowe wspornika D4CS4-FA20.25

Young's modulus, E	167 GPa
Poisson number, ν	0.3
Yield point, R_e	250 MPa
Temporary strength, R_m	400 MPa
Plastic strain at tear, ϵ	15%
Permissible stresses in tension, k_r	65 MPa

Source: own work/ Źródło: opracowanie własne

A simplified front axle bracket model was imported into the ABAQUS program (Fig. 3). That model simplification was aimed to enable dense MES grid generation and to speed up calculations. All casting and technological rounded areas and fillets were removed from the primary model. The left elements included the holes and the areas to be later machined, which had no significant effect on the structural strength of the element.



Source: own work/ Źródło: opracowanie własne

Fig. 2. A CAD model of D4CS4-FA20.25 bracket
Rys. 2. Model CAD wspornika D4CS4-FA20.25

In accordance with the scheme, presented in Figure 2, three forces act on the bracket, whose values are juxtaposed in Table 2. The goal of performed processing was to assess stress distribution in the bracket, with a particular focus on possible stress concentration sites.

Table 2. Specification of D4CS4-FA20.25 bracket loads
Tab. 2. Specyfikacja obciążeń wspornika D4CS4-FA20.25

Load name, designation	Value [N]
Engine weight, N_s	4000
Dead weight, N_0	3300
Front axle reaction, N_c	35000

Source: own work/ Źródło: opracowanie własne

In the Abaqus/CAE environment, stress distribution maps are calculated acc. to the Huber-von Mises-Hencky (HMH) Theory. Following this hypothesis, the measure of material effort is the specific energy of deflection, while the reduced stresses are expressed in the following formula:

$$\sigma_{red} = \sqrt{\frac{1}{2}[(\sigma_1 - \sigma_2)^2 + (\sigma_2 - \sigma_3)^2 + (\sigma_1 - \sigma_3)^2]} \quad (1)$$

where σ_i ($i = 1, 2, 3$) designates subsequent main stresses.

The application of the hypothesis involves checking of the strength condition for uniaxial tension: (k_r designates permissible stresses in tension):

$$\epsilon_{red} \leq k_r, \quad (2)$$

where k_r designates permissible stresses in tension.

The HMH hypothesis is commonly applied in engineering practice and well reflects the actual stress status for a broad group of classical structural materials, such as steel [9]. However, the material of the axle bracket was made of ductile iron, which is accounted to elastic brittle materials [9,14]. Taking that into account, the HMH material effort hypothesis was replaced by the hypothesis of the largest main elongation by de Saint-Venant and Poncelet (SVP) [4,15]. According to that hypothesis, reduced stress is described by the following formula:

$$\sigma_{red} = \sigma_1 - \nu(\sigma_2 - \sigma_3). \quad (3)$$

The strength condition (2) certainly remains valid. However, following the assumptions of the SVP hypothesis, a given element can safely transfer operation loads when the following inequality is met:

$$\varepsilon_{red} \leq \varepsilon_r, \quad (4)$$

where ε_{red} reduced permissible deformation is calculated from the generalised Hook's law, while ε_r designates permissible deformation in tension. It characterises brittle materials very well, as the main feature of brittleness is much lower material resistance to tension than to compression.

The model was digitalised by means of C3D4 tetragonal elements with characteristic size of approximately 7 mm and with bracket overall dimensions of 1080x540x314 mm. Following a convergence study, the grid density with 856043 elements was regarded satisfactory.

3. Calculations

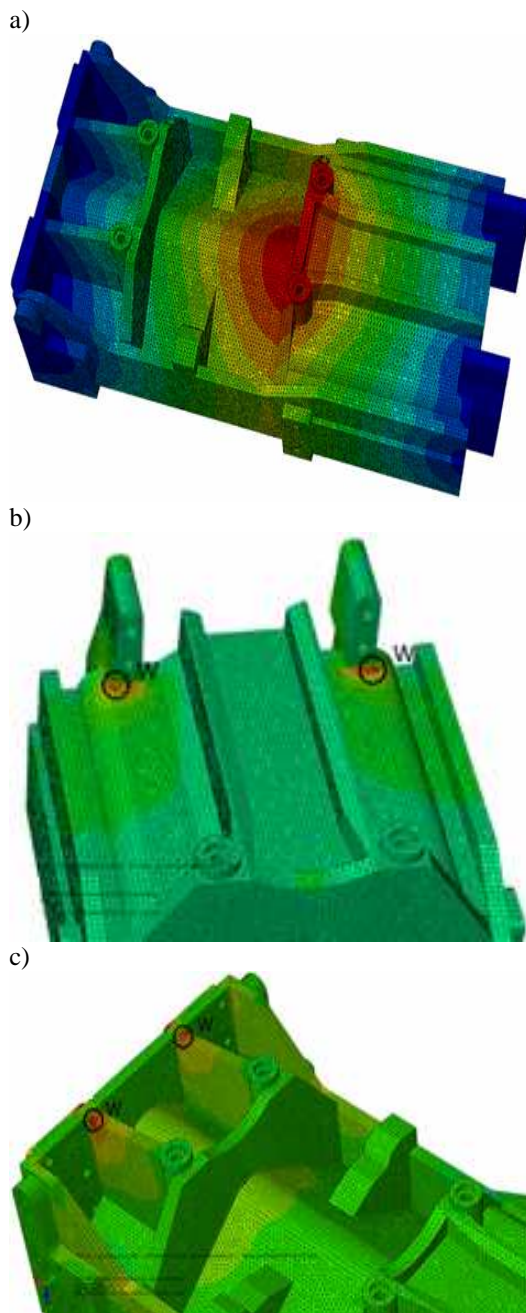
Numerical calculations were run on a Dell T3500 workstation with an Intel Xeon W3540 eight-core processor with CPU speed of 2.93 GHz, 12 GB RAM and RAID-5 array.

Figure 3 presents the stress distributions obtained from data processing. Letter "W" in the Figure designates the sites under the highest stress impacts. The SPV parameter values are marked with colours; the reduced value of this parameter was calculated acc. to formula (3). Figure 3a illustrates stress distribution in the bracket. Analysing that distribution, no stress hazardous sites were identified in the studied bracket. However, an uneven stress distribution was observed around four points of the tractor's axle mounting area. It may then transfer uneven loads onto the axle fixing bolts. The analysis indicated that the potential stress concentration sites occurred at high curvature regions, at the base of the ribs, connecting the bracket with the engine (Fig. 3b). The maximum value of reduced stress σ_{red} was 49 MPa. The permissible limit was not exceeded at that site, however, during tractor operation, bracket cracking at these areas may not be excluded. Therefore, a strengthening of this area is recommended. Figure 3c presents stress distribution in the lower part of the bracket, right at the site of dead weight mounting. Increased stress impacts at that region do not need raise concerns as their level is small ($\sigma_{red}=19$ MPa) vs. other areas of the bracket.

4. Summary

This paper presents the results of a MES analysis of reduced stress distribution, based on the hypothesis of the largest main elongation of de Saint-Venant and Poncelet (SVP) and carried out in a D4CS4-FA20.25 bracket of the front axle of C-380M URSUS tractor. Potential stress concentration areas were identified from performed calculations. No case of exceeding permissible stress level ($k_r = 65$ MPa) was found for the accepted material. The obtained

results indicate the highest stress impacts at the bracket-engine connection area. Therefore, it was recommended to increase rounding radius at highest stress regions. An irregular deformation area was also noted.



Source: own work/ Źródło: opracowanie własne

Fig. 3. Results of stress distribution calculations in D4CS4-FA20.25 bracket a) a view from the side of the axle fixing bolts b) a view of the engine fixing clamps c) a view of the clamps for the front axle weights

Rys. 3. Wyniki obliczeń rozkładu naprężeń w wsporniku D4CS4-FA20.25 a) widok z boku śrub mocujących oś b) widok zacisków mocujących silnik c) widok zacisków dla ciężaru osi przedniej

5. References

- [1] Debski H., Teter A., Kubiak T., Samborski S.: Local buckling, post-buckling and collapse of thin-walled channel section composite columns subjected to quasi-static compression. Composite Structures, 2016, 593-601.

- [2] Dylał Z., Jakubowicz A., Orłoś Z.: Wytrzymałość materiałów, WNT, 2013.
- [3] Ellobody E., Feng R., Young B.: Finite element analysis and design of metal structures. Waltham, MA: Butterworth-Heinemann, 2014.
- [4] Gawęcki A.: Mechanika materiałów i konstrukcji prętowych. Poznań: Alma Mater, 2003.
- [5] German J.: Podstawy i zastosowanie mechaniki pękania w zagadnieniach inżynierskich. Kraków, 2004.
- [6] Guzik E.: Procesy uszlachetniania żeliwa: Wybrane zagadnienia. Katowice: PAN, 2001.
- [7] Hartmann F., Katz C. Structural Analysis with Finite Elements. Berlin, Heidelberg: Springer Berlin Heidelberg, 2007.
- [8] Khennane A.: Introduction to finite element analysis using MATLAB and Abaqus. Boca Raton: CRC Press, 2013.
- [9] Komorzycji C., Teter A.: Podstawy statyki i wytrzymałości materiałów. Lublin: Wydawnictwa Uczelniane PL, 2000.
- [10] Kubiak T., Samborski S., Teter A.: Experimental investigation of failure process in compressed channel-section GFRP laminate columns assisted with the acoustic emission method. Composite Structures, 2015, 921-929.
- [11] Long Y., Cen S., Long Z.: Advanced Finite Element Method in Structural Engineering. Berlin, Heidelberg: Springer Berlin Heidelberg, 2009.
- [12] Turner M.J., Clough R.W., Martin H.C., Topp L.J.: Stiffness and Deflection Analysis of Complex Structures. J. of Aero. Sci., 23 (9), 1956.
- [13] Niezgodziński T., Niezgodziński M.E.: Wytrzymałość materiałów. Wydawnictwo Naukowe PWN, 2009.
- [14] Pietrowski S., Gumienny G.: Ocena jakości żeliwa sferoidalnego EN-GJS-400-15 metodą ATD. Archiwum Odlewnictwa, 2002, 2(6), 257-268.
- [15] Pietrzakowski M.: Wytrzymałość materiałów. Warszawa: Studio MULTIGRAF Sp. z o.o. Company, 2010.
- [16] Rakowski G., Kacprzyk Z.: Metoda elementów skończonych w mechanice konstrukcji. Warszawa: Publishing House of the Warsaw University of Technology, 2016.
- [17] Rusiński E., Czmochoński J., Smolnicki T.: Zaawansowana metoda elementów skończonych w konstrukcjach nośnych. Publishing House of the Wrocław University of Technology, 2000.
- [18] Simulia. Abaqus 6.14. Abaqus/CAE User's Guide. Providence, RI, USA: Dassault Systèmes, 2014.
- [19] Teter A., Debski H, Samborski S.: On buckling collapse and failure analysis of thin-walled composite lipped-channel columns subjected to uniaxial compression. Thin-Walled Structures, 2014, 324-331.
- [20] Zienkiewicz O.C.: Metoda elementów skończonych. Warszawa: Arkady, 1972.